Solution Structures of Mono- and Ditriangular Chini Clusters of Nickel and Platinum. An X-ray Scattering and Quantum Chemical Study

L. Bengtsson-Kloo,*,† C. M. Iapalucci,‡ G. Longoni,*,‡ and S. Ulvenlund§

Inorganic Chemistry 1, Department of Chemistry, Lund University, P.O. Box 124, S-221 00 Lund, Sweden, Diptartimento di Chimica Fisica e Inorganica, Università di Bologna, Viale de Risorgimento 4, I-40136 Italy, and Department of Pharmaceutics, Astra Draco AB, P.O. Box 34, S-221 00 Lund, Sweden

Received September 25, 1997

Results from liquid X-ray scattering show that both $[Ni_6(CO)_{12}]^{2-}$ and $[Pt_6(CO)_{12}]^{2-}$ adopt an overall staggered ditriangular structure of D_3 symmetry in solution. Theoretical calculations show that the energy barrier of rotation is quite small, in particular for the platinum cluster. The possibilities to stabilize monotriangular carbonyl clusters of Ni and Pt in solution were also investigated. Only monotriangular $[Pt_3(CO)_6]^{2-}$ can be stabilized as verified by NMR and IR spectroscopy as well as X-ray scattering. The structure is analogous to that found in the individual triangular units of $[Pt_6(CO)_{12}]^{2-}$, and there is no unambiguous evidence for the need of additional apical CO's to stabilize $[Pt_3(CO)_6]^{2-}$ in solution. Attempts to isolate the corresponding $[Ni_3(CO)_6]^{2-}$ cluster instead produced the very stable $[Ni_5(CO)_{12}]^{2-}$. Mixed solutions of the ditriangular clusters give rise to heteroclusters, whose chemistry is dominated by the facile disproportionation of the Ni_6 clusters.

Introduction

The Chini clusters were first structurally characterized in the middle of the 1970s and consist of triangular $[M_3(CO)_6]_n^{2-}$ cluster fragments ($n \geq 1$) stacked along the 3-fold axis of symmetry.[1−7] The platinum system has been seen to form up to five stacked triangles in $[Pt_3(CO)_6]_5^{2-}$, where the triangles are nearly eclipsed. The stacking of triangular fragments of nickel proceeds in a similar manner up to $[Ni_3(CO)_6]_3^{2-}$, after which the corresponding Ni_{12} cluster exhibits a less regular aufbau. Very large clusters containing up to 30−40 nickel and platinum atoms have also been reported, and the triangular building block motif is still characteristic.[8−11] The chemistry of trimetallic building blocks has recently been nicely highlighted by Imhof and Venanzi.[12] In contrast to nickel and platinum, palladium does not seem to form any stable binary carbonyl clusters; the closest are the mixed phosphine-carbonyl triangular clusters such as $[Pd_3(CO)_3(PPh_3)_3]$, although they have less electrons available for cluster framework bonding than the negatively charged carbonyl clusters of nickel and platinum.[13,14]

The homonuclear and mixed nickel and platinum clusters have also been studied in solution by means of IR spectroscopy and ^{13}C and ^{195}Pt NMR spectroscopy.[15−18] IR spectroscopic data can be used together with the color of the solution as a method of establishing which cluster is predominant in various reaction media. The dynamics of the CO ligands is very fast for the nickel clusters but static enough to allow a good mapping of the isotopomer shifts in ^{13}C and ^{195}Pt spectra of the platinum ones.

The chemistry of triangular clusters of the nickel group of various electron counts has been extensive and include substitution, capping with noble metals and main-group elements and exploration of the redox properties of this class of clusters.[19]

The understanding of the bonding in these triangular cluster building blocks has been enhanced by applied theoretical studies at semiempirical and density-functional level.[20−30] The main difference in bonding between the nickel and platinum clusters is that the d orbitals of Ni tend to be more localized on the metal than those of Pt and thus contribute less to the carbonyl bonding.

The current study concerns the liquid structures of the mono- and ditriangular clusters of nickel and platinum. The reason for our interests is that the monotriangular $[M_3(CO)_6]^{2-}$ building blocks **1** have never been isolated or uniquely structurally

* To whom correspondence should be addressed.
† Lund University.
‡ Università di Bologna.
§ Astra Draco AB.

(1) Calabrese, J. C.; Dahl, L. F.; Chini, P.; Longoni, G.; Martinengo, S. *J. Am. Chem. Soc*. **1974**, *96*, 2614.
(2) Calabrese, J. C.; Dahl, L. F.; Cavalieri, A.; Chini, P.; Longoni, G.; Martinengo, S. *J. Am. Chem. Soc*. **1974**, *96*, 2616.
(3) Longoni, G.; Chini, P. *J. Am. Chem. Soc*. **1976**, *98*, 7225.
(4) Longoni, G.; Chini, P.; Cavalieri, A. *Inorg. Chem*. **1976**, *15*, 3025.
(5) Longoni, G.; Chini, P. *Inorg. Chem*. **1976**, *15*, 3029.
(6) Ceriotti, A.; Chini, P.; ella Pergola, R.; Longoni, G. *Inorg. Chem*. **1983**, *22*, 1595.
(7) Nagaki, D. A.; Lower, L. D.; Longoni, G.; Chini, P.; Dahl, L. F. *Organometallics* **1986**, *5*, 1764.
(8) Ceriotti, A.; Fait, A.; Longoni, G.; Piro, G.; Resconi, L. *J. Am. Chem. Soc*. **1986**, *108*, 5370.
(9) Ceriotti, A.; Demartin, F.; Longoni, G.; Manassero, M.; Marchionna, M.; Sansoni, M. *Angew. Chem., Int. Ed. Engl*. **1985**, *24*, 697.
(10) Mingos, D. M. P.; Wardle, R. W. M. *Trans. Met. Chem*. **1985**, *10*, 441.
(11) Calderoni, F.; Demartin, F.; Iapalucci, M. C.; Longoni, G. *Angew. Chem., Int. Ed. Engl*. **1996**, *35*, 2225.
(12) Imhof, D.; Venanzi, L. M. *Chem. Soc. Rev*. **1994**, 185.
(13) Kudo, K.; Hidai, M.; Uchida, Y. *J. Organomet. Chem*. **1971**, *33*, 393.
(14) Burrows, A. D.; Mingos, D. M. P. *Trans. Met. Chem*. **1993**, *18*, 129.
(15) Brown, C.; Heaton, B. T.; Chini, P.; Fumagalli, A.; Longoni, G. *J. Chem. Soc., Chem. Commun*. **1977**, 309.
(16) Brown, C.; Heaton, B. T.; Towl, A. D. C.; Chini, P.; Fumagalli, A.; Longoni, G. *J. Organomet. Chem*. **1979**, *181*, 233.
(17) Longoni, G.; Heaton, B. T.; Chini, P. *J. Chem. Soc., Dalton Trans*. **1980**, 1537.
(18) Ceriotti, A.; Demartin, F.; Longoni, G.; Manassero, M.; Piva, G.; Piro, G.; Sansoni, M.; Heaton, B. T. *J. Organomet. Chem*. **1986**, *301*, C5.

S0020-1669(97)01229-9 CCC: $15.00
Published on Web 08/07/1998

characterized. We are therefore interested to investigate whether they can be synthesized and stabilized in solution at all, and whether additional carbonyls will be required.

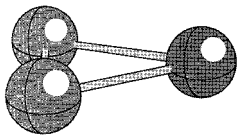

1

In the solid state the $[M_3(CO)_6]_2^{2-}$ clusters of Ni and Pt differ in that the nickel cluster has the triangular subunits in a staggered conformation **2** (D_{3d} symmetry) whereas the platinum one has them in a nearly eclipsed geometry **3** (D_{3h} symmetry; in the crystal structure the cluster is only slightly distorted by a translational displacement along one triangular Pt−Pt edge).

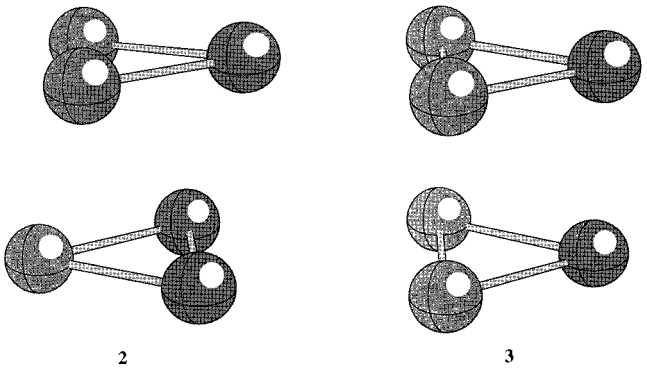

2 **3**

The larger $[M_3(CO)_6]_n^{2-}$ clusters also display an ambiguity concerning the stacking of the triangular subunits. In $[Pt_3(CO)_6]_3^{2-}$ the triangles are twisted with respect to each other around the pseudo-C_3 axis by about 13°.[1] The corresponding nickel cluster is less regular, showing twisting angles of 9 and 21° with respect to the central triangular subunit.[7] The $[Pt_3(CO)_6]_4^{2-}$ and $[Pt_3(CO)_6]_5^{2-}$ clusters can be considered to be formed by capping the $[Pt_3(CO)_6]_3^{2-}$ cluster with one and two triangles, respectively.[1,3] The twisting angles of the terminal triangular fragments are less than 10° but are almost 30° within the central $[Pt_3(CO)_6]_3^{2-}$ unit. The corresponding $[Ni_{12}(CO)_{21}]^{2-}$ cluster deviates from the overall pattern of triangle stacking by forming the larger (also triangularly shaped) $Ni_6(CO)_9$ unit capped by two $Ni_3(CO)_6$ triangles in a staggered conformation.[6] The intertriangular nonbonding repulsion between adjacent subunits is expected to be higher in such a cluster. The existing structural data thus indicate that steric effects from the CO ligands can be of importance for the cluster conformation. Furthermore, in solution static packing effects are absent and we wish to examine if the conformations of the $[M_3(CO)_6]_2^{2-}$ clusters also differ under such conditions and to estimate the intertriangular potential surface, thus estimating the energy required for rotational deformation of the triangular stacks from the ideal conformations shown in **2** and **3**. The mixed $[Ni_3Pt_3(CO)_{12}]^{2-}$ cluster has been proposed, on the basis of NMR spectroscopic evidence, to form in solution, and we also intend to seek structural verification of this observation.

Table 1. CO Stretch Frequencies Observed in the IR Spectra

solution	frequencies[a]/cm^{-1}
0.62 M $Na_2[Ni_3(CO)_6]$ in THF/HMPA	1922 (s), 1952 (s)
0.37 M $Na_2[Pt_3(CO)_6]$ in THF/HMPA	1739 (s), 1945 (vs)
0.31 M $(Me_4N)_2[Ni_6(CO)_{12}]$ in DMF	1785 (s), 1810 (m), 1983 (vs)
0.12 M $Na_2[Pt_6(CO)_{12}]$ in DMF	1800 (s), 1822 (m), 2000 (vs)
0.12 M $(Me_4N)_2[Ni_6(CO)_{12}]$ and 0.12 M $(Me_4N)_2[Pt_6(CO)_{12}]$ in DMF	1796 (s), 1815 (m), 1991 (vs)

[a] m = medium; s = strong; vs = very strong.

The strategy of investigation was to prepare the mono- and ditriangular clusters in solution at a concentration of ca. 0.1 M or higher and then to analyze them by liquid X-ray scattering (LXS), supported by IR, Raman, and multinuclear NMR spectroscopy and quantum chemical calculations at Hartree−Fock and density-functional levels. The quantum chemical analysis also makes it possible to extend the discussion from purely structural to also involve energetic reasoning.

Experimental Section

Synthesis. The $[M_6(CO)_{12}]^{2-}$ clusters (M = Ni, Pt) were synthesized in DMF solution according to the route described previously.[31] To maximize the concentration of the cluster in solution, Na^+ and $(CH_3)_4N^+$ were used as cations. The concentration of the clusters and other physical data are summarized in Table 2. Further reduction to form the monotriangular $[M_3(CO)_6]^{2-}$ clusters was achieved using CO over Na or Na/K alloy. However, a solvent with better electron-solvating power was required and a mixture of HMPA (**caution!** *HMPA is carcinogenic.*) and THF (1:2) was chosen. The monotriangular clusters (especially that of nickel) are extremely sensitive to air and moisture.

Vibrational Spectroscopy. The IR spectra were recorded on a Nicolet 20SXC FT-IR spectrometer. Together with the characteristic color the IR spectra served as important indicators for the major cluster products of reaction. In particular, the CO-stretch region represents a sensitive tool for the identification of the different Chini clusters (see Table 1).

The Raman spectra were recorded on a Bruker IFS66/FRA106 FT-Raman spectrometer, employing the exciting radiation of a YAG laser

(19) See for instance the references below and the reviews 9, 11, and 13: (a) Briant, C. E.; Gilmour, D. I.; Mingos, D. M. P.; Wardle, R. W. M. *J. Chem. Soc., Dalton Trans.* **1985**, 1693. (b) Briant, C. E.; Wardle, R. W. M.; Mingos, D. M. P. *J. Organomet. Chem.* **1984**, *267*, C49. (c) Payne, N. C.; Ramachandran, R.; Schoettel, G.; Vittal, J. J.; Puddephatt, R. J. *Inorg. Chem.* **1991**, *30*, 4048. (d) Mingos, D. M. P.; Wardle, R. W. M. *J. Chem. Soc., Dalton Trans.* **1986**, 73. (e) Burrows, A. D.; Jeffrey, J. G.; Machell, J. C.; Mingos, D. M. P. *J. Organomet. Chem.* **1991**, *406*, 399. (f) Albinati, A.; Moor, A.; Pregosin, P. S.; Venanzi, L. M. *J. Am. Chem. Soc.* **1982**, *104*, 7672. (g) Albinati, A.; Dahmen, K.-H.; Demartin, F.; Forward, J. M.; Longley, C. J.; Mingos, D. M. P.; Venanzi, L. M. *Inorg. Chem.* **1992**, *31*, 2223. (h) Jennings, M. C.; Shoettel, G.; Roy, S.; Puddephatt, R. J.; Douglas, G.; Manojlovic-Muir, L.; Muir, K. W. *Organometallics* **1991**, *10*, 580. (i) Spivak, G. J.; Hao, L.; Vittal, J. J.; Puddephatt, R. J. *J. Am. Chem. Soc.* **1996**, *118*, 225. (j) Hao, L.; Vittal, J. J.; Puddephatt, R. J. *Inorg. Chem.* **1996**, *35*, 269. (k) Stockhammer, A.; Dahmen, K. H.; Gerfin, T.; Venanzi, L. M.; Gramlich, V.; Petter, W. *Helv. Chim. Acta* **1991**, *74*, 989. (l) Hallam, M. F.; Howells, N. D.; Mingos, D. M. P.; Wardle, R. W. M. *J. Chem. Soc., Dalton Trans.* **1985**, 845. (m) Ling, S. S. M.; Hadj-Bagheri, N.; Manojlovic-Muir, L.; Muir, K. W.; Puddephatt, R. J. *Inorg. Chem.* **1987**, *26*, 231.
(20) Chang, K. W.; Woolley, R. G. *J. Phys., Ser. C* **1979**, *12*, 2745.
(21) Evans, J.; *J. Chem. Soc., Dalton Trans.* **1980**, 1005.
(22) Pacchioni, G.; Fantucci, P.; Valenti, V. *J. Organomet. Chem.* **1982**, *224*, 89.
(23) Fantucci, P.; Pacchioni, G.; Valenti, V. *Inorg. Chem.* **1984**, *23*, 247.
(24) Underwood, D. J.; Hoffmann, R.; Tatsumi, K.; Nakamura, A.; Yamamoto, Y. *J. Am. Chem. Soc.* **1985**, *107*, 5968.
(25) Pacchioni, G.; Fantucci, P. *Chem. Phys. Lett.* **1987**, *134*, 407.
(26) Mingos, D. M. P.; Slee, T. *J. Organomet. Chem.* **1990**, *394*, 679.
(27) Pacchioni, G.; Rösch, N. *Inorg. Chem.* **1990**, *29*, 2901.
(28) Rösch, N.; Ackermann, L.; Pacchioni, G. *J. Am. Chem. Soc.* **1992**, *114*, 3549.
(29) Pacchioni, G.; Ackermann, L.; Rösch, N. *Gazz. Chim. Ital.* **1992**, *122*, 205.
(30) Pacchioni, G.; Rösch, N. *Acc. Chem. Res.* **1995**, *28*, 390.
(31) (a) Ceriotti, A.; Longoni, G.; Piva, G. *Inorg. Synth.* **1989**, *26*, 312. (b) Ceriotti, A.; Longoni, G.; Marchionna, M. *Inorg. Synth.* **1989**, *26*, 316.

Table 2. Atom Concentrations and Physical Data of the Cluster Solutions Analyzed by LXS

parameters	Ni_6[a]	Pt_6[b]	Pt_6/Ni_6[c]	Ni_3[d]	Pt_3[e]
C_{Pt}/M		0.74	0.71		1.12
C_{Ni}/M	1.88		0.71	1.86	
C_P/M				2.42	2.49
C_{Na}/M		0.25		1.24	0.74
C_O/M	14.42	12.98	13.63	10.96	9.70
C_N/M	11.28	11.51	11.28	7.24	7.47
C_C/M	38.24	35.99	37.13	37.53	37.10
C_H/M	82.13	80.54	81.32	82.10	84.68
V/Å^3 [f]	884.22	2250.09	2355.41	892.78	1487.96
ρ/g cm^{-3}	1.041	1.032	1.083	1.023	1.103
μ/cm^{-1} [g]	5.9	17.0	18.2	6.4	25.9
s_{exp}/Å^{-1} [h]	0.0 − 13.1	0.0 − 13.1	0.0 − 13.1	0.0 − 13.1	0.0 − 13.1
s_{lsf}/Å^{-1} [i]	3.0 − 12.5	3.0 − 12.5			5.0 − 12.5
r_{corr}/Å[j]	0.80	0.80	0.80	0.85	0.80
k[k]	0.008	0.008	0.008	0.008	0.008

[a] 0.31 M $(Me_4N)_2[Ni_6(CO)_{12}]$ in DMF. [b] 0.12 M $Na_2[Pt_6(CO)_{12}]$ in DMF. [c] 0.12 M $(Me_4N)_2[Ni_6(CO)_{12}]$ and 0.12 M $(Me_4N)_2[Pt_6(CO)_{12}]$in DMF. [d] Formal concentration of 0.62 M $Na_2[Ni_3(CO)_6]$ in THF/HMPA. [e] 0.37 M $Na_2[Pt_3(CO)_6]$ in THF/HMPA. [f] Stoichiometric volume per Pt or Ni atom. [g] Linear absorptivity. [h] Experimental range in s. [i] Range of s used in the least-squares refinement. [j] Value of r under which spurious peaks were removed by a reverse FT procedure. [k] Damping factor in function $\exp(-ks^2)$ for the FT.

(1064 nm). The spectra turned out to be less informative than expected because of the very intense color of the concentrated cluster solutions.

NMR Spectroscopy. The ^{1}H, ^{13}C, ^{17}O, ^{61}Ni, and ^{195}Pt spectra of the cluster solutions were recorded on a Varian Unity 300 MHz spectrometer. Only the ^{13}C and ^{195}Pt spectra turned out to carry any useful structural information, and the ^{13}C chemical shifts are given with respect to TMS and those of ^{195}Pt with respect to the fixed frequency 64.2 MHz (normalized to a proton frequency of 300 MHz).

Liquid X-ray Scattering. The X-ray scattering of the solutions optimized in cluster concentration was recorded at room temperature using a solid-state Ge detector mounted on a Seifert GSD $\theta-\theta$ diffractometer. The samples were confined in sealed 1 mm Lindemann capillaries, and the scattered radiation was recorded in the range $0.6 \leq \theta \leq 48.0°$ in steps of $s = 0.0335$ ($s = 4\pi\lambda^{-1} \sin\theta$). The reproducibility was checked by repeated scans. 40 000 counts were collected at each point in the θ range below 34.375° and 20 000 counts above, using Mo Kα radiation (0.7107 Å). The observed intensities were corrected for background radiation, Compton scattering, polarization, the solutions with linear absorption higher than 15 cm^{-1} also for multiple scattering, and finally normalized to the theoretical independent scattering from a stoichiometric unit volume, V. Spurious peaks below about 0.8 Å were removed by a Fourier re-transformation procedure. The data treatment has been described in detail before.[32,33] The concentrations and physical data of the cluster-containing solutions studied are given in Table 2. All data corrections and calculations were made using the program Kurvlr.[34]

The scattering data can be analyzed both qualitatively and quantitatively. In the comparison with structural models obtained from analogous systems (solid or liquid) or quantum chemical calculation, much information can be extracted from the number of major peaks in the reduced radial distribution function (rRDF), corresponding to atom−atom distances, and their relative intensity. The exact position of the peaks in the rRDF is not the target of such a qualitative analysis. Nevertheless, this type of simple comparisons often provides essential information about the chemistry of a system. For qualitatively good models or systems with rRDF's dominated by a few strong peaks, also a quantitative analysis providing more exact atom−atom distances, temperature coefficients and number of atom−atom correlations can be performed by means of a least-squares procedure. The iterative least-squares fit of a structural model was made on the corrected intensity data by means of the program Steplr.[35] The effective s ranges used in the least-squares fits are given in Table 2. Also the pure solvents, DMF and THF/HMPA, were studied and used in the evaluation of the cluster structural data.

Theoretical Calculations. The quantum chemical calculations in this work were made with the Gaussian92/94 package.[36] Several basis sets were initially tested, and the best combination of calculational accuracy and effort was provided by standard 3-21G for C and O, and the average relativistic effective core potential (ARECP) basis sets by Stevens and co-workers;[37−40] the 3-21G basis sets can be described as (6s6p)/[3s3p] for C and O and the basis sets of Stevens and co-workers employ a 60-electron ARECP for Pt and 10-electron one for Ni, and the valence space is essentially (7s7p5d)/[4s4p3d] and (8s8p6d)/[4s4p3d] for Pt and Ni, respectively.

Although these basis sets are of moderate size, they amount to about 400 basis functions and 800 primitives for the largest systems studied. For this reason, full optimizations of the $[M_6(CO)_{12}]^{2-}$ clusters within the D_{3d} and D_{3h} symmetries were only performed at Hartree−Fock (HF) level. The intratriangular parameters were then kept constant and the intertriangular distances optimized at density-functional level (SVWN and B3LYP) in order to observe the effect of electron correlation. The monotriangular $[M_3(CO)_6]^{2-}$ clusters were fully optimized at both HF and various density-functional levels. The calculations within the density-functional formalism were performed both using the local density approximation (SVWN),[41] nonlocal corrections to the exchange and correlation functionals (BLYP)[42] and finally also Becke's three-parameter hybrid method (B3LYP).[43] The choice of these functionals represents an increase in formal sophistication of how the electron correlation is handled; the hybrid method B3LYP has by experience turned out to work quite well for many inorganic and organometallic systems.

(32) Ulvenlund, S.; Bengtsson, L. A. *J. Mol. Struct.* **1994**, *326*, 181.
(33) Bengtsson, L. A. Ph.D. Thesis, Lund University, Sweden, 1990.
(34) Johansson, G.; Sandström, M. *Chem. Scr.* **1973**, *4*, 195.
(35) Molund, M.; Persson, I. *Chem. Scr.* **1985**, *25*, 197.
(36) Frisch, M. J.; Trucks, G. W.; Schlegel, H. B.; Gill, P. M. W.; Johnson, B. G.; Robb, M. A.; Cheeseman, J. R.; Keith, T. A.; Petersson, G. A.; Montgomery, J. A.; Raghavshari, K.; Al-Laham, M. A.; Zakrzewski, V. G.; Ortiz, J. V.; Foresman, J. B.; Cioslowski, J.; Stefanov, B.; Nanayakkara, A.; Challacombe, M.; Peng, C. Y.; Ayala, P. Y.; Chen, W.; Wong, M. W.; Andres, J. L.; Replogle, E. S.; Gomperts, R.; Martin, R. L.; Fox, D. J.; Binkley, J. S.; Defrees, D. J.; Baker, J.; Stewart, J. P.; Head-Gordon, M.; Gonzalez, C.; Pople, J. A. *Gaussian92/94*, Gaussian Inc.: Pittsburgh, PA, 1995.
(37) Binkley, J. S.; Pople, J. A.; Hehre, W. J. *J. Am. Chem. Soc.* **1980**, *102*, 939.
(38) Gordon, M. S.; Binkley, J. S.; Pople, J. A.; Pietro, W. J.; Hehre, W. J. *J. Am. Chem. Soc.* **1982**, *104*, 2797.
(39) Pietro, W. J.; Francl, M. M.; Hehre, W. J.; Defrees, D. J.; Pople, J. A.; Binkley, J. S. *J. Am. Chem. Soc.* **1982**, *104*, 5039.
(40) Stevens, W. J.; Krauss, M.; Basch, H.; Jasien, P. G. *Can. J. Chem.* **1992**, *70*, 612.
(41) (a) Slater, J. C. In *Quantum Theory of Moleculesand Solids*, McGraw-Hill: New York, 1974; Vol. 4. (b) Vosko, S. H.; Wilk, L.; Nusair, M. *Can. J. Phys.* **1980**, *58*, 1200.
(42) (a) Becke, A. D.; *Phys. Rev., Ser. A* **1988**, *38*, 3098. (b) Lee, C.; Yang, W.; Parr, R. G. *Phys. Rev., Ser. B* **1988**, *37*, 785.
(43) Becke, A. D.; *J. Chem. Phys.* **1993**, *98*, 5648.

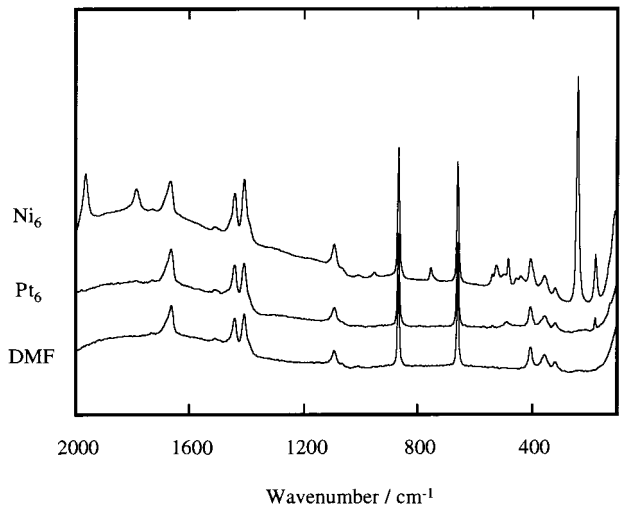

Figure 1. FT Raman spetra of $[Ni_6(CO)_{12}]^{2-}$ and $[Pt_6(CO)_{12}]^{2-}$ in DMF and of the solvent DMF itself.

Results and Discussion

$[M_6(CO)_{12}]^{2-}$ Clusters. The cluster-containing solutions studied by X-ray scattering were also subjected to Raman, IR, and NMR spectroscopic investigations. The Raman spectra turned out to be less informative than expected because of the very intense color of the solutions. Figure 1 only allows speculation in terms of a cluster mixture present or low cluster symmetry for the solution formally containing $[Ni_6(CO)_{12}]^{2-}$.

The ^{13}C and ^{195}Pt NMR and IR spectra essentially reproduce already known data, however, important from an analytical point of view when extending our study to invoke X-ray scattering.[15−18] The ^{195}Pt spectrum of the solution containing $[Pt_6(CO)_{12}]^{2-}$ consists of a singlet as expected, and the isotopomer pattern of the ^{13}C spectrum in Figure 2a is analogous to that detected by Heaton and co-workers. It should be pointed out that the chemical shift pattern emerges from intratriangular platinum isotope effects alone, since ^2J couplings between the Pt_3 triangles seems to be effectively decoupled by intertriangular dynamics.

The corresponding ^{13}C spectrum of the solution containing $[Ni_6(CO)_{12}]^{2-}$, shown in Figure 2b, only displays two broad signals because of CO scrambling; the signal from bridging CO's is at the higher positive chemical shift. A weak but distinct peak from apical CO's in $[Ni_5(CO)_{12}]^{2-}$ can also be discerned at +205 ppm. This weak peak and the absence of any detectable signals in the Raman and IR spectra indicate that the solution only is contaminated by a small amount of $[Ni_5(CO)_{12}]^{2-}$.

The data from LXS measurements are not straightforward to analyze for these systems. The metal−metal correlations are readily observed in the rRDF's, but structural models based on the ideal conformations shown in **2** and **3** fail to properly model the structural features of the $[M_3(CO)_6]_2^{2-}$ clusters in solution. As indicated by the Raman and NMR spectroscopic results, the DMF solution seems to contain only $[Pt_6(CO)_{12}]^{2-}$. The interpretation of the scattering data from the corresponding $[Ni_6(CO)_{12}]_2^{2-}$ solution is complicated by the lower scattering power of nickel and the presence of $[Ni_5(CO)_{12}]^{2-}$.

Results from a quantum chemical analysis was therefore undertaken in order to obtain nonbiased structural models for the $[M_3(CO)_6]_2^{2-}$ clusters in the solutions studied. Both $[Ni_6(CO)_{12}]^{2-}$ and $[Pt_3(CO)_{12}]^{2-}$ were fully optimized at HF level. The optimization was performed within the C_{2v} point group in order to detect any tendency to intratriangular deviation from ideal D_{3h} symmetry. According to Pyykkö the interaction

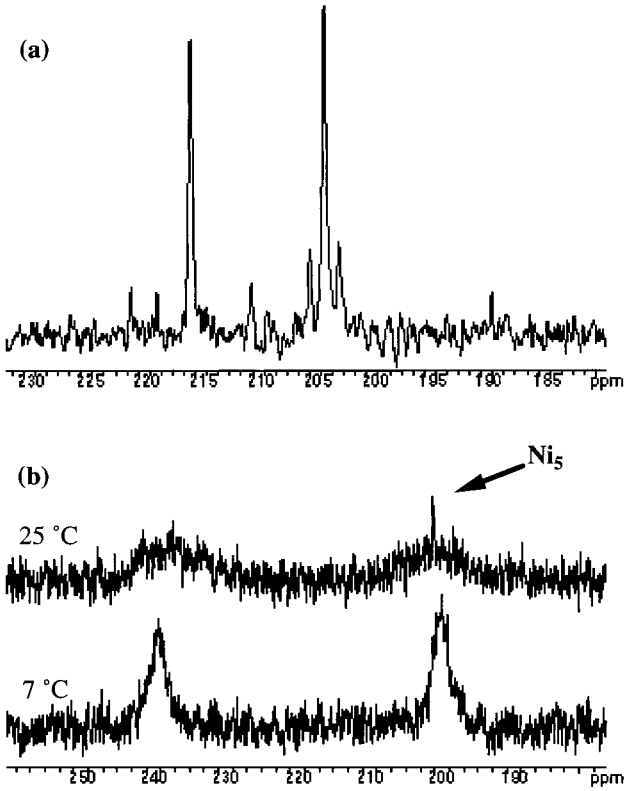

Figure 2. Natural abundance ^{13}C spectra of (a) $[Pt_6(CO)_{12}]^{2-}$ in DMF and (b) $[Ni_6(CO)_{12}]^{2-}$ in DMF at 7 and 25 °C.

between the triangular units is substantially supported by correlation effects (i.e. dispersion forces).[44] For this reason we also performed partial optimizations of the intertriangular distances for the ideal geometries with D_{3h} and D_{3d} symmetry (corresponding to 0 and 60° rotational deformation in our formalism, respectively) at SVWN and B3LYP levels, as well as intermediate rotational conformers of D_3 symmetry at B3LYP level, to invoke effects from electron correlation. Apart from tabulated calculational data given, it should be mentioned that the CO ligands have a tendency to bend out of the triangular plane away from the cluster center; terminal CO's typically by 2−3° and bridging ones by as much as 5−7°.

The crystal structures made us expect either the D_{3h} or D_{3d} conformation (most likely the latter) to predominate in solution. Indeed, the theoretical calculations at HF level show that the D_{3d} conformation is favored by 18 and 5 kJ mol^{-1} for the Ni_6 and Pt_6 clusters, respectively. Inclusion of correlation increases the stability of the D_{3d} relative the D_{3h} conformation to 26 and 79 kJ mol^{-1} for $[Ni_6(CO)_{12}]^{2-}$ at SVWN and B3LYP level, respectively. For $[Pt_6(CO)_{12}]^{2-}$ the energy differences are much smaller and although the D_{3d} configuration is favored by 21 kJ mol^{-1} at SVWN level, it is disfavored by 3 kJ mol^{-1} at B3LYP level. To put these values into perspective, one should bear in mind that the thermal energy at room temperature is almost 3 kJ mol^{-1} and that the systematic calculational error probably is of the magnitude 10 kJ mol^{-1}.

Since the structural parameters provided by the B3LYP calculations are in good general agreement with known experimental data, we pursued the study of rotational energy differences at this level. The intertriangular distance was optimized at intertriangular angles of 0 (D_{3h}), 10, 20, 30, 40, 50, and 60° (D_{3d}) and the energy thus determined. The energy

(44) Pyykkö, P.; *Chem. Rev.* **1997**, *97*, 597.

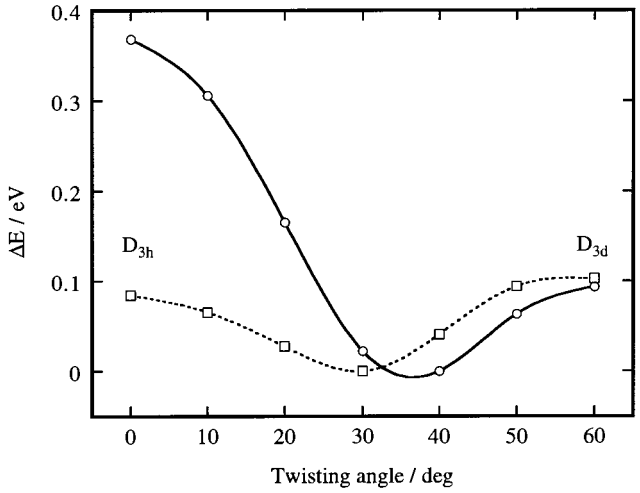

Figure 3. Relative energy vs twisting angle for $[Pt_3(CO)_6]_2^{2-}$ (circles; solid line) and $[Ni_3(CO)_6]_2^{2-}$ (squares; dotted line).

vs angle for the nickel and platinum clusters is displayed in Figure 3. Unexpectedly, the ideal conformations of D_{3h} and D_{3d} symmetry are transition states in both systems, and the true minimum corresponds to a twisting angle of about 30° (37° for the Ni_6 and 30° for the Pt_6 cluster, respectively), as shown in **4**.

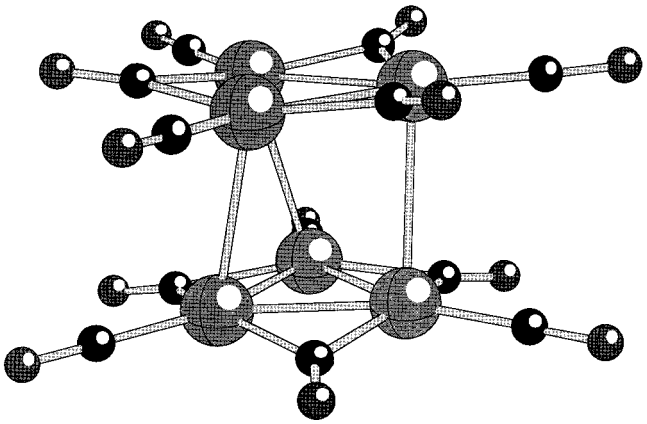

4

Again, the energy differences are rather small, especially for the platinum cluster, and the relevance of these results can be challenged. However, the rRDF of the $[Pt_6(CO)_{12}]^{2-}$ solution is almost perfectly matched by the calculational results, as shown in Figure 4a. The results of a least-squares fit based on this structural model is displayed in Figure 4b and Table 3. Although the information about approximate Pt−C correlations can be extracted from solution data, they are heavily affected by any mismatch in the Pt−Pt envelope. Therefore, the Pt−C and Pt−O distances used in the least-squares analysis were taken from the solid compounds and kept invariant during the evaluation of the Pt−Pt parameters. The same structural model is applicable to the $[Ni_6(CO)_{12}]^{2-}$ solution, and a reasonable fit is obtained. However, the Ni−Ni correlation observed at 2.8 Å in Figure 4c is most likely due to the apical-equatorial Ni−Ni distance in $[Ni_5(CO)_{12}]^{2-}$.

It should be pointed out that the structure shown in **4** is the overall staggered one, in which all metal atoms and CO ligands are in a staggered conformation with respect to each other. As mentioned above, dispersion effects together with the steric repulsion and electronic interaction are three factors that

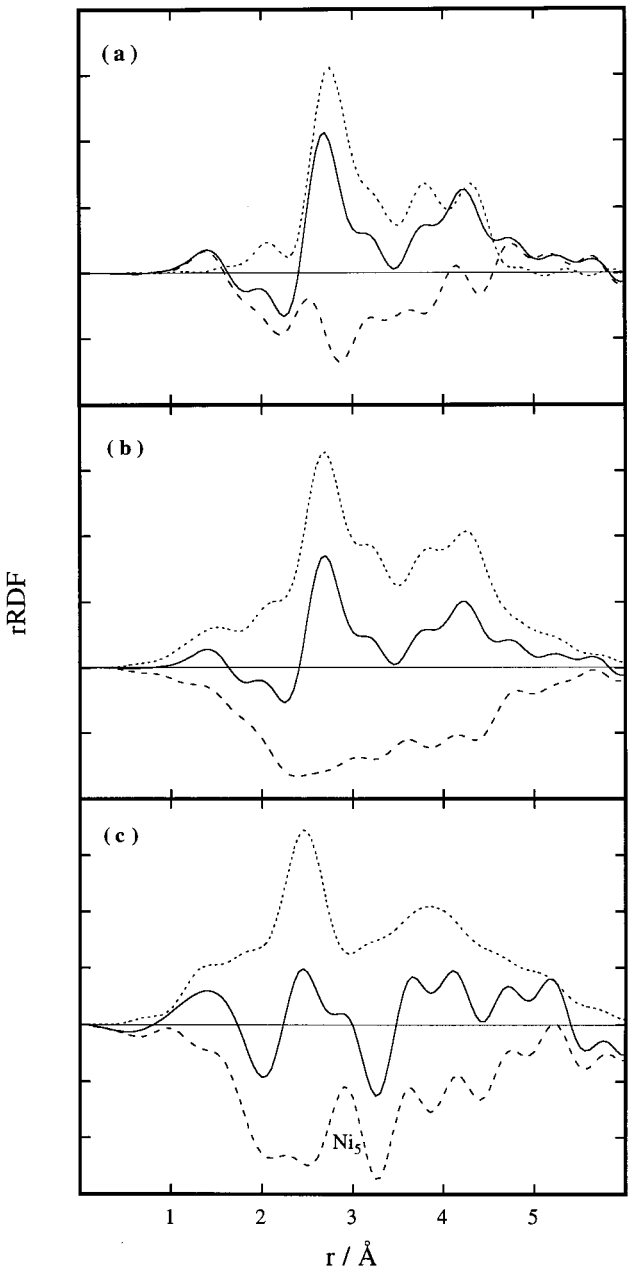

Figure 4. rRDF for (a) DMF solution of $[Pt_6(CO)_{12}]^{2-}$ with the structural model directly taken directly from the theoretical structure optimized at B3LYP level of D_3 symmetry; (b) DMF solution of $[Pt_6(CO)_{12}]^{2-}$ with the structural model obtained by a least-squares fit, in which the number of Pt−Pt vectors deviate less than 20% from the theoretically expected ones; (c) DMF solution of $[Ni_6(CO)_{12}]^{2-}$ with a structural model obtained by a least-squares fit, although the data are strongly interfered by the presence of $[Ni_5(CO)_{12}]^{2-}$. Experimental data are shown by a solid, structural model by a dotted curve and the difference by a hatched curve in all figures.

determine the final conformation of the ditriangular clusters; not to mention packing effects in the solids. On the basis of LDA level DFT calculations Pacchioni and Rösch compared the intertriangular interaction in $[Ni_6(CO)_{12}]^{2-}$ to hydrogen bonding, rather than invoking direct metal−metal covalent bonding, since the bond energy was estimated to 20 kJ mol^{-1} or less per Ni−Ni contact (of which there are six in D_{3d} conformation).[30] Concludingly, the present results indicate that nonbonding steric effects together with the strong dispersion character of the intertriangular interaction give rise to the D_3 staggered conformation on the expense of direct covalent metal−

Table 3. Calculated and Experimental Structural Data for the Ditriangular Chini Clusters of Nickel and Platinum

cluster	symmetry	method	$d_{M-Mintra}$/Å	d_{M-Ct}/Å	d_{M-Cb}/Å	d_{Ct-Ot}/Å	d_{Cb-Ob}/Å	$d_{\Delta-\Delta}$/Å	$d_{M-Minter}$/Å
$Ni_6(CO)_{12}^{2-}$	D_{3d}	HF[a]	2.416	1.814	1.904	1.140	1.178	2.804	3.133, 3.956
		SVWN						2.276	2.669, 3.600
		B3LYP						2.600	2.950, 3.813
		LXS[b]	2.42 (0.005)	1.75	1.90			2.65	2.75, 3.31, 3.86 (0.01)
		solid[c]	2.38	1.75	1.90	1.13	1.17	2.41	2.77, 3.65
	D_3(30°)	B3LYP						2.660	2.756, 3.312, 3.787
$Ni_6(CO)_{12}^{2-}$	D_{3h}	HF	2.418	1.808	1.908	1.143	1.174	3.018	3.018, 3.867
		SVWN						2.571	2.571, 3.529
		B3LYP						2.833	2.833, 3.763
$Pt_6(CO)_{12}^{2-}$	D_{3d}	HF[a]	2.722	1.930	2.109	1.143	1.167	3.120	3.575, 4.481
		SVWN						2.657	3.087, 4.116
		B3LYP						2.997	3.384, 4.343
		LXS[b]	2.68 (0.005)	1.77	2.03			3.02	3.14, 3.76, 4.25 (0.01)
	D_3(30°)	B3LYP						3.035	3.142, 3.760, 4.291
$Pt_6(CO)_{12}^{2-}$	D_{3h}	HF	2.719	1.931	2.107	1.144	1.166	3.282	3.281, 4.262
		SVWN						2.889	2.889, 3.969
		B3LYP						3.134	3.134, 4.151
		solid[d]	2.66	1.77	2.03	1.23	1.21	3.04	3.04, 4.04

[a] The formal D_{3d} structures were optimized within C_{2v} in order to detect tendencies of deviation. Distances averaged to D_{3d}. [b] Only metal−metal distances can be determined with acceptable accuracy; temp. coefficients in brackets (Å^2); M−C distances taken from solid. [c] From ref 2. [d] From ref 1, idealized to D_{3h} symmetry.

metal bonding in solution. Because of the small energy differences involved, packing effects and cation−anion interaction in solid compounds can very well push the structure toward any of the two extremes of D_{3h} or D_{3d} symmetry.

The equimolar mixture of $[Ni_6(CO)_{12}]^{2-}$ and $[Pt_6(CO)_{12}]^{2-}$ gives rise to two singlets of equal intensity about 25 ppm apart in the ^{195}Pt NMR spectrum. The peak at lower chemical shift can be identified as arising from $[Pt_6(CO)_{12}]^{2-}$, whereas the other was interpreted as emerging from statistical mixing of M_3 triangular units to form a 1:2:1 ratio of $[Ni_6(CO)_{12}]^{2-}/[Ni_3Pt_3(CO)_{12}]^{2-}/[Pt_6(CO)_{12}]^{2-}$, in which the mixed cluster is assumed to give rise to the new peak at about +20 ppm.[16] Schematically this can be formulated according to

$$Pt_6 + Ni_6 \rightarrow 2Pt_3Ni_3 \quad (1)$$

In this context it is interesting to note that the CO-stretch frequencies in the IR spectra of the mixture are intermediate to those of the pure cluster solutions (Table 1). However, the initially observed signals, attributed to $[Ni_3Pt_3(CO)_{12}]^{2-}$ and $[Pt_6(CO)_{12}]^{2-}$, lose their intensity with time and several new signals, which cannot be readily interpreted, develop over a period of several hours. All attempts to isolate the suggested $[Ni_3Pt_3(CO)_{12}]^{2-}$ species were unsuccessful. Precipitation upon layering of isopropyl alcohol of the above 1:1 mixtures of $[Ni_6(CO)_{12}]^{2-}$ and $[Pt_6(CO)_{12}]^{2-}$ in acetone gave rise to crystal mixtures of $[Ni_6Pt_6(CO)_{21}]^{4-}$ and $[Ni_5Pt_7(CO)_{21}]$.[4-45] Both compounds display solid-state structures analogous to that of $[H_{4-n}Ni_9Pt_3(CO)_{21}]^{n-}$ (n = 2, 3, 4),[18] with the extra platinum atoms randomly distributed over the six sites of the two outer $M_3(CO)_6$ triangles.[46] Such species should display rather characteristic nonbinomial multiplets in their platinum NMR spectra due to coupling between nonequivalent atoms, of which there is no evidence in the spectra of the above $[Ni_6(CO)_{12}]^{2-}/[Pt_6(CO)_{12}]^{2-}$ acetone mixtures.

Although the initial study was performed in acetone, we observe the analogous behavior in DMF solution. However, the rRDF of an equimolar mixture closely resembles that of $[Pt_6(CO)_{12}]^{2-}$ (see Figure 5). In fact, the subtraction of all platinum from the rRDF in the form of Pt_6 leaves a difference

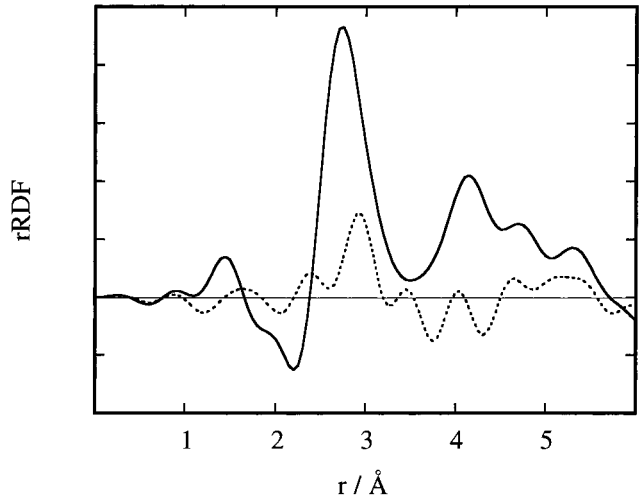

Figure 5. rRDF of the 1:1 mixture of $[Pt_6(CO)_{12}]^{2-}$ and $[Ni_6(CO)_{12}]^{2-}$ in DMF. The hatched curve represents the original rRDF subracted with that of pure $[Pt_6(CO)_{12}]^{2-}$ normalized to one Pt per stoichiometric volume.

rRDF rather similar to that of the Ni_6 solution. LXS data thus indicate that whatever happens in solution, the Pt_6 core is left unchanged. Therefore, the intial model proposed ought to be modified. Considering all available data, an alternative model such as eq 2 may be conceivable. The modified model (eq 2)

$$[Ni_6(CO)_{12}]^{2-} + [Pt_6(CO)_{12}]^{2-} \rightleftharpoons [Ni_6Pt_6(CO)_{24}]^{4-} \xrightarrow[\text{slow}]{} [Ni_6Pt_6(CO)_{21}]^{4-} + 3CO \quad (2)$$

provides a rational interpretation of both NMR and IR spectroscopic as well as the LXS results. Indeed, at least two ^{195}Pt singlets would be expected: one for unreacted $[Pt_6(CO)_{12}]^{2-}$ and a second for a $[Ni_6Pt_6(CO)_{24}]^{4-}$ species generated by sandwiching the former within two $Ni_3(CO)_6$ moieties, in which all platinum atoms are equivalent. In such a case the rRDF would be dominated by the structural features of the Pt_6 core, as it has been experimentally found. Moreover, the suggested $[Ni_6Pt_6(CO)_{24}]^{4-}$ intermediate would possess two extra valence electrons and its slow rearrangement by loss of carbon monoxide to the final $[Ni_6Pt_6(CO)_{21}]^{4-}$ product would be understandable.

(45) Marchionna, M. Ph.D. Thesis, University of Milan, Italy, 1986.
(46) Manassero, M. Personal communication.

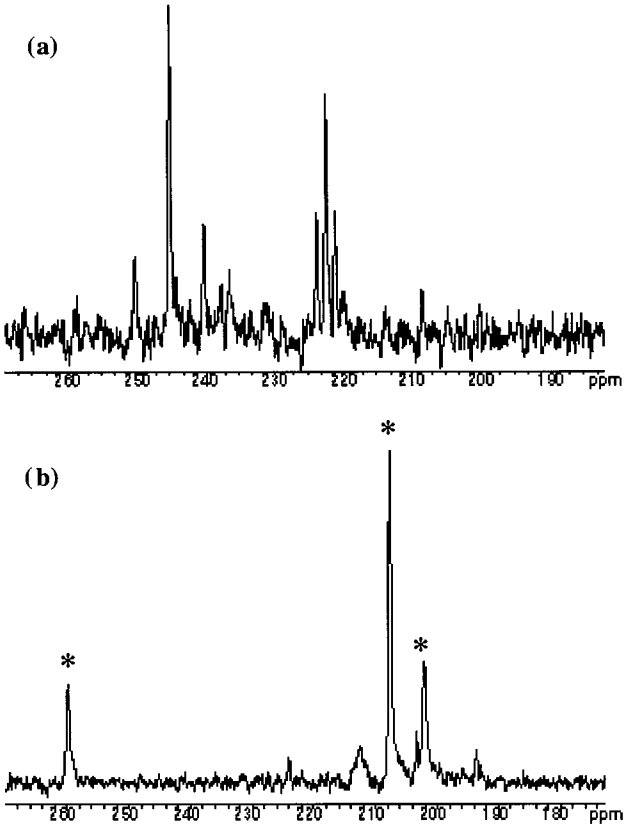

Figure 6. Natural abundance ^{13}C spectra of (a) $[Pt_3(CO)_6]^{2-}$ in THF/HMPA; and (b) formal $[Ni_3(CO)_6]^{2-}$ in THF/HMPA.

$[M_3(CO)_6]^{2-}$ Clusters. The potassium salt of the $[Pt_3(CO)_6]^{2-}$ dianion was isolated only as powder and characterized by elemental analysis and IR spectroscopy.[3] We prepared the $[Pt_3(CO)_6]^{2-}$ dianion by reduction of $[NMe_4]_2[Pt_6(CO)_{12}]$ with Na/K alloy in a fairly good electron-solvating mixture of THF and HMPA. As shown in Figure 6, the ^{13}C isotopomer NMR spectrum of the above fuchsia solution is analogous to that $[Pt_6(CO)_{12}]^{2-}$. The chemical shifts of both terminal and bridging carbonyls are expectedly shifted up in frequency with respect to those of $[Pt_6(CO)_{12}]^{2-}$ due to the higher free negative charge per metal atom, whereas the observed coupling constants ($^1J(Pt-C_t) = 2109$, $^2J(Pt-C_t) = 197$, and $^1J(Pt-C_b) = 752$ Hz) are consistent with the corresponding values of the latter.

The rRDF of this solution (Figure 7) can be readily interpreted in view of the results previously discussed. The formal Pt_3 solution indeed predominantly contains the monotriangular $[Pt_3(CO)_6]^{2-}$ cluster with the structure shown in **5** (or in a "naked" form, **1**).

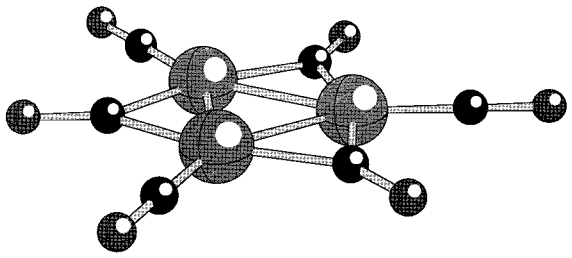

5

With regard to nickel the situation is less straightforward. The synthesis of a $[Ni_3(CO)_8]^{2-}$ species has been reported to occur via a reduction of $Ni(CO)_4$ with NaOH in methanol or lithium amalgam in THF.[47,48] No solution IR data for this species, which has been suggested to consist of a Ni_3 triangle capped above and below by two face-bridging carbonyls, are available. In our hands, both the above synthetic procedures afford solutions mainly containing $[Ni_6(CO)_{12}]^{2-}$. The salts of the latter are rather renitent to reduction under a nitrogen atmosphere; these can be reduced in HMPA with a solution of sodium in HMPA directly to a dark species showing infrared carbonyl absorptions at ca. 1890 and 1750 cm^{-1}. The observed CO frequencies are not comparable with those of $[Pt_3(CO)_6]^{2-}$ and are too low to be caused by a nickel congener of the latter.

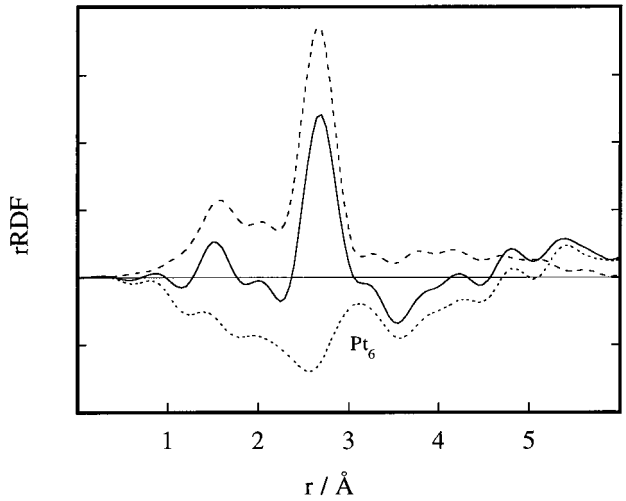

Figure 7. rRDF of $[Pt_3(CO)_6]^{2-}$ in THF/HMPA.

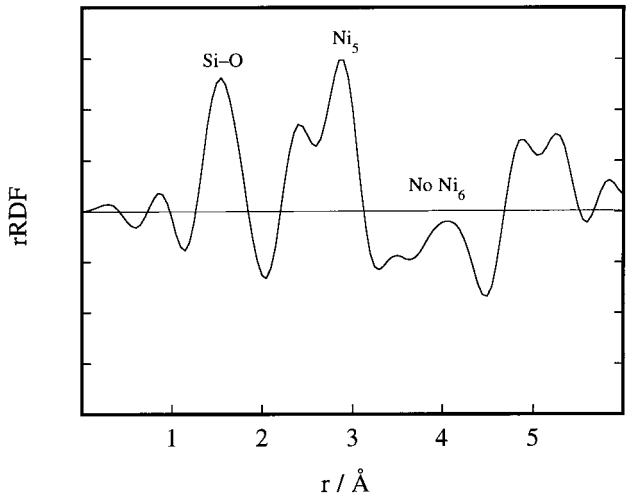

Figure 8. rRDF of formal $[Ni_3(CO)_6]^{2-}$ in THF/HMPA.

In contrast, the $[Ni_6(CO)_{12}]^{2-}$ and $[Ni_5(CO)_{12}]^{2-}$ salts are readily reduced both in THF with a solution of sodium in naphthalene, or in HMPA with sodium to give a fuchsia compound only displaying terminal carbonyl absorptions at 1952 and 1922 cm^{-1}. No other infrared carbonyl absorptions are present down to ca. 1500 cm^{-1}. This same compound precipitate from the solution as red-violet leaflets on pressurizing a saturated THF solution of $(NMe_4)_2[Ni_5(CO)_{12}]$ under anhydrous conditions at 4−6 atm with carbon monoxide. Analysis of these crystals is in keeping with a $(NMe_4)[Ni_3(CO)_9]$ composition, which would imply a structure based on an open Ni_3 triangle.

(47) Sternberg, H. W.; Markby, R.; Wender, I. *J. Am. Chem. Soc.* **1960**, *82*, 3639.
(48) Hieber, W.; Ellerman, J. *Z. Naturforsch., Ser. B* **1963**, *18*, 595.

Table 4. Calculated and Experimental Structural Data for the Monotriangular Chini Clusters of Nickel and Platinum

cluster	symmetry	method	$d_{M-Mintra}$/Å	d_{M-Ct}/Å	d_{M-Cb}/Å	d_{Ct-Ot}/Å	d_{Cb-Ob}/Å
$Ni_3(CO)_6^{2-}$	D_{3h}	HF	2.411	1.780	1.905	1.152	1.181
		SVWN	2.313	1.702	1.856	1.193	1.212
		BLYP	2.419	1.756	1.917	1.204	1.223
		B3LYP	2.389	1.743	1.901	1.188	1.208
$Pt_3(CO)_6^{2-}$	D_{3h}	HF	2.706	1.913	2.097	1.153	1.176
		SVWN	2.664	1.851	2.047	1.190	1.210
		BLYP	2.766	1.900	2.104	1.202	1.221
		B3LYP	2.727	1.890	2.089	1.186	1.206
		LXS[a]	2.66 (0.005)	1.77	2.03		
$Ni_5(CO)_{12}^{2-}$	C_{3v}	HF	2.405, 2.951	1.830, 1.810	1.898	1.138, 1.152	1.182[d]
		B3LYP	2.394, 2.797	1.753, 1.790	1.902	1.176, 1.182	1.198[d]
		LXS[a,b]	2.40, 2.87 (0.005, 0.008)				
		solid[b,c]	2.36, 2.81	1.857, 1.756	1.840	1.038, 1.153	1.132[d]

[a] Only metal−metal distances can be determined with acceptable accuracy; temp. coefficients in brackets (Å^2); M−C distances taken from solid structures. [b] Equatorial and apical distances given for Ni−Ni and Ni−C_t. [c] From ref 49. [d] Equatorial distances given first, and whenever relevant apical ones.

Unfortunately, the fuchsia solutions of this compound immediately turn yellow-brown in the presence of trace amounts of oxygen or moisture, due to its ready conversion into $[Ni_5(CO)_{12}]^{2-}$.

In the attempt to gain some better insight into the nature of this fuchsia species, we have subjected its THF/HMPA solutions to ^{13}C NMR spectroscopy and LXS. The results show that the stabilization of a Ni_3 monotriangular cluster is far from straightforward. As shown in Figure 6, the ^{13}C NMR spectrum of the formal Ni_3 solution distinctly shows that it consists predominantly of $[Ni_5(CO)_{12}]^{2-}$. The remaining peaks do not contain enough information to allow any assignments. Accordingly, the rRDF of the formal Ni_3 solution (Figure 8) only gives evidence for $[Ni_5(CO)_{12}]^{2-}$, **6**. Furthermore, the latter rRDF is blurred by an artifact arising from the glass walls of the Lindeman capillaries. These failures stem from the difficulties found in safely handling this compound in solution, since it is tremendously sensitive to the traces of humidity present on the walls of the sample holders and the equipment for transferring solutions.

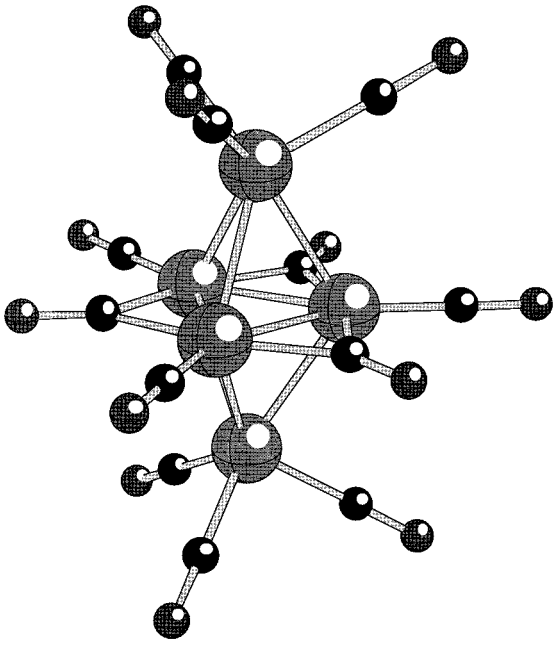

6

The results of quantum chemical calculations, collected in Table 4, show that both the $[Ni_3(CO)_6]^{2-}$ and $[Pt_3(CO)_6]^{2-}$ clusters are electronically stable at both HF and density-functional level. However, in real life we have so far only succeeded in stabilizing the Pt_3 cluster thermodynamically, whereas the Ni_3 congener falls into the thermodynamic pitfall of $[Ni_5(CO)_{12}]^{2-}$. It is still not known whether additional CO's are needed to stabilize the M_3 clusters. IR spectroscopic data of reaction solutions have been interpreted in terms of a $[Ni_3(CO)_8]^{2-}$ cluster **7**, with two apical CO's on each side of the Ni_3 cluster. From a calculational point of view the results

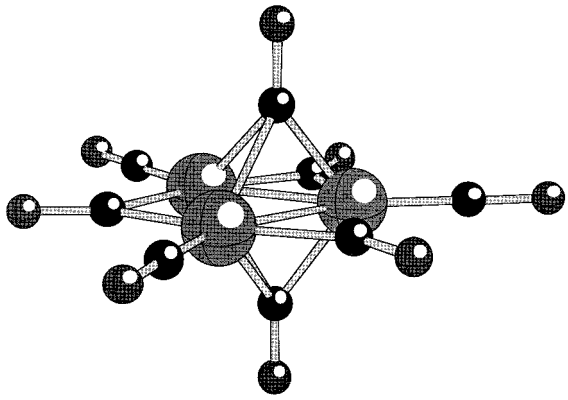

7

for the $[M_3(CO)_6]^{2-}$ clusters offer a potential problem: the HOMO's have positive energy (about 3−4 eV) at all levels of calculation. Considering that the HOMO essentially consist of metal p orbitals perpendicular to the M_3 plane, bridging CO's may provide additional stability to the monotriangular clusters. However, only extra CO's according to **7** give reasonable optimized M−C distances and the resulting HOMO's are still positive. The structure **8** with a single apical CO does not seem

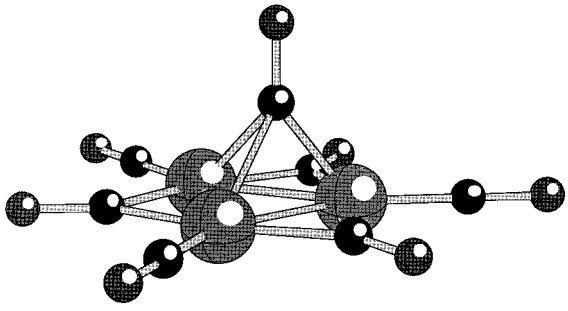

7

to be a feasible proposition, since the CO in all cases is pushed

away from the triangular plane to distances above 4 Å. The fact that the HOMO's have positive energies is of course nonphysical, but the inclusion of positive charges or potassium cations 5 Å above and below the mass entre of the M_3 triangle shows that the electrostatic field created is large enough to push the energies of the HOMO's to negative values; this situation most likely more adequately mimics the actual situation in solution.

So far, we do not have any evidence of the occurrence in solution of tight ion-pairing similar to the kind observed, for instance, for the alkali salts of $[Co_3(CO)_9(\mu_3\text{-}CO)]^-$,[49] and such a possibility appears rather unlikely in view of the ionizing power of HMPA. However, in apparent agreement with the ion-pairing hypothesis, we have obtained spectroscopic evidence of the possible stabilization of a $[Ni_3(CO)_3(\mu\text{-}CO)_3]^{2-}$ moiety by interaction with a formal I^+ ion.[50] Indeed, the formation of a green-brown byproduct which appears to be $[Ni_3(CO)_3(\mu\text{-}CO)_3I]^-$ has been observed both in the degradation of $[Ni_9(CO)_{18}]^{2-}$ with I^- or I_2, as well as in the reaction of $Ni(CO)_4$ with I^- to give $[Ni(CO)_3I]^-$. This species shows the characteristic IR pattern of the $[M_3(CO)_3(\mu\text{-}CO)_3]_n^{2-}$ aggregates, and the crude product give analytical results in reasonable agreement with the suggested formula. Unfortunately, also this suggested trinuclear species is not stable enough in solution to allow a more complete characterization.

Consequently, there is neither theoretical nor experimental evidence for additional CO's, or other ligands, providing an extra energetical stabilization for the M_3 monotriangular clusters.

Conclusions

The present results indicate that the ditriangular clusters $[M_6(CO)_{12}]^{2-}$ (M = Ni, Pt) have a preferred conformation in which the triangular subunits are twisted about 30° with respect to one another in solution, although the energy barrier of rotation is quite small in both clusters. The structural results obtained for the equimolar mixture of the $[Ni_6(CO)_{12}]^{2-}$ and $[Pt_6(CO)_{12}]^{2-}$ clusters are consistent with a disproportionation of the Ni_6 cluster to form heteronuclear clusters with a retained Pt_6 core. The monotriangular clusters $[M_3(CO)_6]^{2-}$ (M = Ni or Pt) are much more difficult to stabilize, and in solution only the Pt_3 cluster can be unambiguously identified. The monotriangular platinum cluster is structurally very similar to those found in $[Pt_6(CO)_{12}]^{2-}$. There is no conclusive evidence for the need of apical CO's to stabilize the monotriangular clusters.

Acknowledgment. This work has been supported by the Swedish National Science Research Council and the Human Capital and Mobility (contract no. CHRX CT93 0277). The PDC at the Royal Institute of Technology in Stockholm is acknowledged for their allocation of computer resources, and the Crafoord Foundation for financial support allowing upgrading of existing workstations.

IC971229R

(49) Facchinetti, G.; Fochi, G.; Funaioli, T.; Zanazzi, P. F. *Angew. Chem., Int. Ed. Engl.* **1987**, *26*, 680 and references therein.

(50) Lower, L.; Dahl, L. F.; Longoni, G.; Chini, P. *J. Am. Chem. Soc.* **1975**, *97*, 5034.